JOURNAL OF CATALYSIS **163,** 158–168 (1996)
ARTICLE NO. 0315

NO Decomposition over Mn_2O_3 and Mn_3O_4

Tatsuji Yamashita and Albert Vannice

Department of Chemical Engineering, The Pennsylvania State University, University Park, Pennsylvania 16802-0044

Received March 4, 1996; revised May 16, 1996; accepted May 28, 1996

Mn_2O_3 is better than Mn_3O_4 for catalytic NO decomposition; regardless, appreciable activities were not observed below 773 K. For example, at 0.040 atm NO and 773 K, Mn_2O_3 had a specific activity of 3.5×10^{-4} μmole N_2/s/m^2 and an activation energy of 11 kcal/mole, while for Mn_3O_4 comparable values were 6.5×10^{-5} μmole N_2/s/m^2 and 15 kcal/mole, respectively. Based on NO chemisorption at 300 K, these specific activities correspond to turnover frequencies of 7.5×10^{-5} s^{-1} and 1.6×10^{-5} s^{-1} for Mn_2O_3 and Mn_3O_4, respectively. Pretreatment in He at 873 K produced more O_2 desorption from Mn_2O_3 (6.1 molecules O_2/m^2) than from Mn_3O_4 (2.2 molecules O_2/m^2), but no changes in either XRD pattern were detected. Consequently, oxygen vacancies were formed and, as in previous studies, activity is associated with these vacancies. Reaction orders on NO ranged from 1.4 to 1.9 between 833 and 873 K, with the higher values occurring with O_2 in the feed. Negative reaction orders on O_2 were around -0.3 and not strongly dependent on temperature. A Langmuir–Hinshelwood model involving a surface reaction between two adsorbed NO molecules fit the data well and gave kinetic parameters which provided the following values: for the reaction between two adsorbed NO molecules, $E_a = 46$ kcal/mole; for NO adsorption, $\Delta H^o_{ad} = -25$ kcal/mole and $\Delta S^o_{ad} = -25$ cal/mole/K; for O_2 adsorption, $\Delta H^o_{ad} = -35$ kcal/mole and $\Delta S^o_{ad} = -31$ cal/mole/K. A comparison to specific activities obtained from the literature for oxides showed the following order at 773 K:

$$Cu/ZSM\text{-}5 \gg Co_3O_4 > La_2O_3 \simeq Mn_2O_3 > CuO > NiO,\ Fe_2O_3.$$

INTRODUCTION

NO is the major component of NO_x, which exists in waste gas from power plants, motor vehicles, and virtually any combustion process. NO_x has been considered as a pollutant which contributes to acid rain, urban smog, and stratospheric ozone depletion (1). Past efforts on the abatement of NO_x have led to the development and commercialization of selective catalyst reduction (SCR) using ammonia; however, SCR has inherent problems related to its usage of NH_3, which is hazardous in itself and environmentally unacceptable (2). With growing concern about environmental pollution along with more stringent regulations on NO_x emissions, continuing efforts have been made to improve NO_x abatement technology. Catalytic NO_x abatement is one of the solutions, and two major methods have been investigated—they are direct NO_x decomposition to N_2 and O_2 and NO_x reduction using reducing agents other than NH_3 (3). If possible, direct NO_x decomposition is more desirable because it does not require any foreign compounds. Various materials, which include metals and metal oxides, have been examined as catalysts for the decomposition of NO; however, only three studies have attempted to investigate NO decomposition over any Mn oxide. None has reported any kinetic data, thus no information is available regarding kinetic parameters, catalytic behavior, or specific activities related to this reaction on Mn oxide surfaces. Therefore, this study examines the catalytic activity of Mn oxides, chiefly Mn_2O_3 and Mn_3O_4, compares their catalytic behavior, measures NO chemisorption, and proposes a reaction mechanism based on detailed kinetic data obtained with the most active Mn oxide—Mn_2O_3.

EXPERIMENTAL

The unsupported Mn oxides used, Mn_2O_3 (34.4 m^2/g) and Mn_3O_4 (21.9 m^2/g), were the same as those used in a previous N_2O decomposition study (4); i.e., they were single-phase, crystalline powders obtained from Chemetals Incorporated. Equipment and procedures used for the measurements of surface areas and XRD patterns of Mn oxides also have been described previously (4).

Catalyst pretreatment before either reaction or chemisorption experiments was conducted *in situ* in a quartz tube reactor or a quartz adsorption cell by exposing the oxide to He at 1 atm and 10 ml/min. The temperature was raised from room temperature to 873 K at a rate of 10 K/min and held there for 1 h. During some of the pretreatment runs, the O_2 released from the Mn oxides was monitored by gas chromatography.

Chemisorption of NO and O_2 was carried out at 300 K using a UHV volumetric system (4). The sample size was 1 g, and equilibrium partial pressures of NO and O_2 up to 200 Torr were used. Because slow NO adsorption occurred after a rapid initial uptake, pressure measurement of each experimental point for NO adsorption was made after 90 min of contact time, while 30 min was enough for O_2 adsorption.

0021-9517/96 $18.00

Catalytic activity measurements for the NO decomposition reaction were conducted at atmospheric pressure in a microreactor under steady-state conditions. The reactor and the peripherals were interconnected mostly with 1/8″ stainless steel tubing and Swagelok connections, and the diameter in the middle of the reactor, a 7-mm i.d. quartz tube, was constricted to ~4 mm to support quartz wool on which catalyst samples were loaded (5). Typically, 4.04% NO in He was passed downward at a total flow rate of 10 ml/min through the reactor which contained 0.5 g catalyst (GHSV $\simeq$ 1500 h^{-1}). Concentrations and flow rates of the feed gas were governed by Tylan mass flow controllers. The reactor was vertically inserted into the opening of a solid stainless-steel insert which was placed inside a tube furnace (Hoskins Electric Furnace, FD-303-A). The stainless steel insert increased thermal conductivity and improved temperature uniformity. The pressure drop across the reactor was around 0.04 atm with little variation between reaction temperatures of 773 to 873 K and an outlet pressure of 0.97 atm. A K-type thermocouple was inserted directly into the catalyst bed to obtain accurate temperature measurements, and temperature was kept within $\pm 1^{\circ}$ by an Omega CN2011 temperature controller. It was confirmed that without catalyst no decomposition of NO occurs up to 873 K in this reactor. The conversion of NO was routinely kept below 7%; i.e., a differential reactor mode was maintained to minimize any complications which could arise from mass and heat transfer limitations. The Weisz criterion (6) for second-order reactions showed that internal diffusion effects were not important (5). All the gases used were UHP grade from MG Industries except for two NO/He mixtures: one was 4.04% NO in He which contained 360 ppm N_2 and 170 ppm N_2O as major impurities, and the other was 4660 ppm NO in He which contained 70 ppm N_2 as the major impurity.

Product analyses were made with gas chromatography (GC) using a 5A molecular sieve column, and NO conversions were also determined with a NO_x analyzer (5). The sampling valve and 1/8″ stainless steel line from the reactor to the valve was kept at 373 K to avoid condensation of any NO_2 formed. The temperature program used (an initial hold for 5 min at 323 K, heating to 533 K at a rate of 35 K/min, and then holding 2 min at 533 K) enabled separation of O_2, N_2, NO, and N_2O, but quantitative analysis of NO_2 was not possible with this setup. A typical gas chromatogram is shown elsewhere (5). When O_2 coexisted in the feed gas, the effluent gas from the reactor contained significant amounts of O_2 which interfered with the NO peak by forming NO_2 and made NO analysis inaccurate; therefore, catalyst activity was expressed by the rate of N_2 formation. Most of the N_2O existing as an impurity in the 4.04% NO/He mixture decomposed and produced N_2, and that amount as well as the N_2 impurity in the feed gas was subtracted when calculating the net effluent N_2 concentration.

As it was impossible to determine NO_2 concentration in the effluent gas by gas chromatography, a NO_x chemiluminescence analyzer (Lear Siegler ML 9841 Analyzer) was used for that purpose. When the sample contained NO_2, it was passed through a converter containing Mo shavings which reduced NO_2 into NO before the sample was contacted with ozone. The difference in chemiluminescence with and without the usage of the converter gives the NO_2 concentration. The NO_x analyzer was calibrated by standard gases of 100 ppm NO in He and 10 ppm NO_2 in He. Because the maximum detection limit of this analyzer was 100 ppm NO_x, the effluent gas from the reactor at 100 ml/min was diluted with 4000 ml/min of prepurified-grade N_2 which had been stripped of water by a Drierite trap and of hydrocarbons by an activated carbon trap.

RESULTS

A working temperature range of 773–873 K was required for sufficiently high NO conversions, which necessitated a catalyst pretreatment at 873 K or higher for stable catalytic performance. To check the effect of pretreatment temperature, samples of Mn_2O_3 were heated at 873, 923, or 973 K for 1 h under He at 10 ml/min and atmospheric pressure, which resulted in a decrease in the surface area of Mn_2O_3 from 34.4 m^2/g to 30.6, 27.3, or 17.4 m^2/g, respectively. The pretreatment at 923 K gave a slight brownish tint to the catalyst on top of the original black, and the pretreatment at 973 K clearly turned the top quarter of the catalyst bed brown, while the pretreatment at 873 K showed no apparent changes. As shown in Fig. 1, after the 973 K pretreatment changes appeared in the XRD pattern of the catalyst that were ascribable to the Mn_3O_4 phase, while no detectable changes were observed after the other pretreatments. Hence, the pretreatment temperature was selected to be 873 K for Mn_2O_3 as well as Mn_3O_4, which is more stable to temperature changes. No change in the XRD pattern was observed for Mn_3O_4 after the 873 K pretreatment. As before, O_2 released during pretreatment of Mn_2O_3 and Mn_3O_4 at 873 K was monitored, and Fig. 2 plots the O_2 concentration in the effluent gas and the temperature in the catalyst bed during the pretreatment of these two oxides. The resolution was not especially good because continuous GC measurements were not possible; however, multiple desorption peaks were still observable for both Mn_2O_3 and Mn_3O_4. Amounts of O_2 released were estimated by integrating the areas under the curves, and these values along with the BET surface are given in Table 1. Nominal formulae for Mn_2O_3 and Mn_3O_4 after the 873 K pretreatment were $Mn_2O_{2.90}$ and $Mn_3O_{3.98}$, respectively, which indicates that substantial amounts of lattice oxygen were removed.

As observed before, MnO_2 converted into Mn_2O_3 when it was pretreated at 773 K, and MnO_2 and Mn_2O_3 pretreated at 773 K gave approximately the same specific activity for

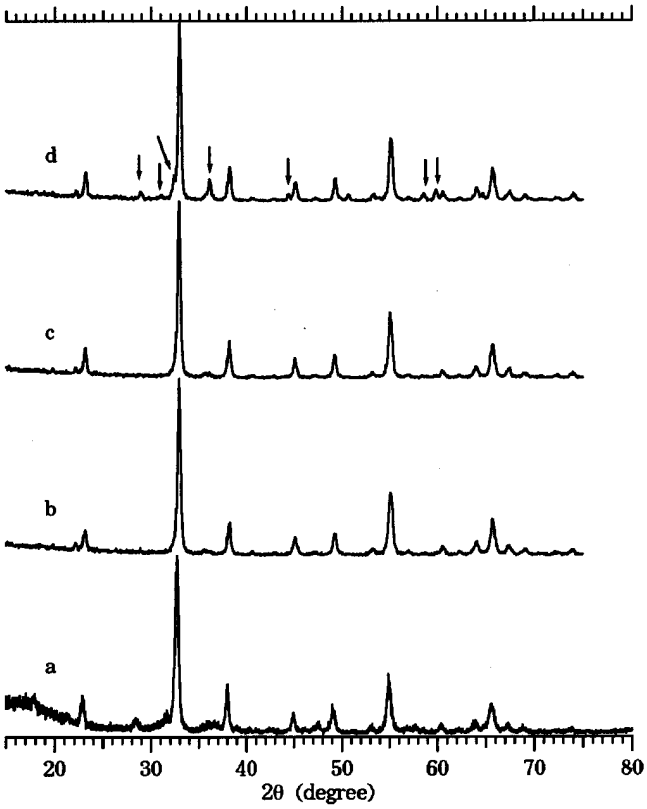

FIG. 1. XRD patterns of Mn_2O_3 before (a) and after pretreatment at: (b) 873 K, (c) 923 K, and (d) 973 K. The arrows identify peaks from Mn_3O_4.

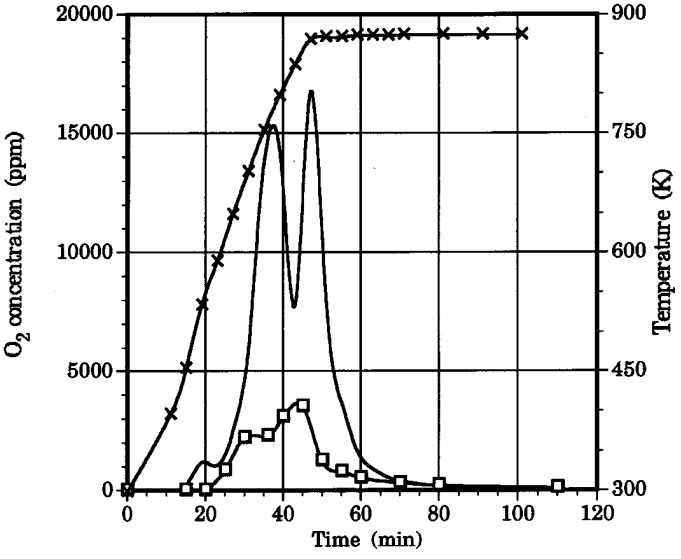

FIG. 2. O_2 concentration in the effluent gas during pretreatment of Mn_2O_3 and Mn_3O_4 under 10 ml/min of helium: (—) Mn_2O_3, 0.46 g; (□) Mn_3O_4, 0.55 g; (×) temperature.

NO decomposition at 773 K and 0.04 atm of NO (5); consequently, further examination of MnO_2 was abandoned because of the high temperatures required. Studies with MnO were not conducted because it is oxidized by NO, even at 300 K (7). When NO decomposition over Mn_2O_3 and Mn_3O_4 was carried out without O_2 in the feed, no O_2 was observed in the effluent gas by GC, whereas N_2 was observed. The NO decomposition activity of Mn_2O_3 was monitored versus time on stream, and its deactivation was determined at both 873 K and 0.04 atm of NO and 833 K and 0.02 atm of NO. The results are shown in Fig. 3 as a change in relative activity based on the activity given. If the rapid activity decreases during the first hour are neglected, activity losses amounted to 15% during 12 h on stream at 833 K and 12% during 6 h on stream at 873 K. The gradual decrease may be due in part to the sintering of Mn_2O_3 because the surface area dropped to 26.8 m^2/g at 873 K and to 28.6 m^2/g at 833 K. XRD patterns showed no observable changes in the bulk phases.

Figure 4 shows Arrhenius plots for NO decomposition over Mn_2O_3 and Mn_3O_4 between 773 and 873 K with either 0.02 or 0.04 atm of NO. Activity measurements were made after several hours on stream with both ascending and descending temperatures, and the results showed that little catalyst deactivation occurred during these runs. The apparent activation energies for NO decomposition over Mn_2O_3 and Mn_3O_4 were 11 and 15 kcal/mol, respectively, at either pressure. On a surface area basis, Mn_3O_3 was about four times as active as Mn_3O_4. Activities at 873 K were also measured at various partial pressures of NO between 0.0023 and 0.04 atm for Mn_2O_3 and between 0.013 and 0.04 atm for Mn_3O_4, and again no appreciable catalyst deactivation was

TABLE 1

Effect of Catalyst Pretreatment on Surface Area, O_2 Desorption, and Chemisorption

	Pretreatment temp. (K)	Mn_2O_3	Mn_3O_4
Surface area[a]			
m^2/g	None	34.4	21.9
	773	31.8	18.7
	873	30.6	18.3
O_2 release during pretreatment			
μmol/g	773	170	41
	873	310	67
μmol/m^2	773	5.3	2.2
	873	10.1	3.7
molecule/$m^2 \times 10^{18}$	773	3.2	1.3
	873	6.1	2.2
Irreversible O_2 uptake			
μmol/m^2	873	0.32	0.07
molecule/$m^2 \times 10^{18}$	873	0.19	0.04
Irreversible NO uptake			
μmol/m^2	873	4.7	4.1
molecule/$m^2 \times 10^{18}$	873	2.8	2.5

[a] Surface areas used for the measurement of O_2 release.

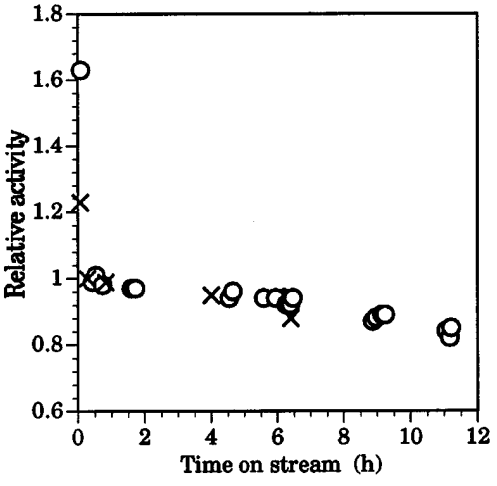

FIG. 3. Activity maintenance with Mn_2O_3: (○) 833 K, 0.02 atm NO (final surface area, 28.6 m^2/g), activity basis 2.5×10^{-4} μmol N_2/s-m^2; (×) 873 K, 0.04 atm NO (final surface area, 26.8 m^2/g), activity basis 8.1×10^{-4} μmol N_2/s-m^2.

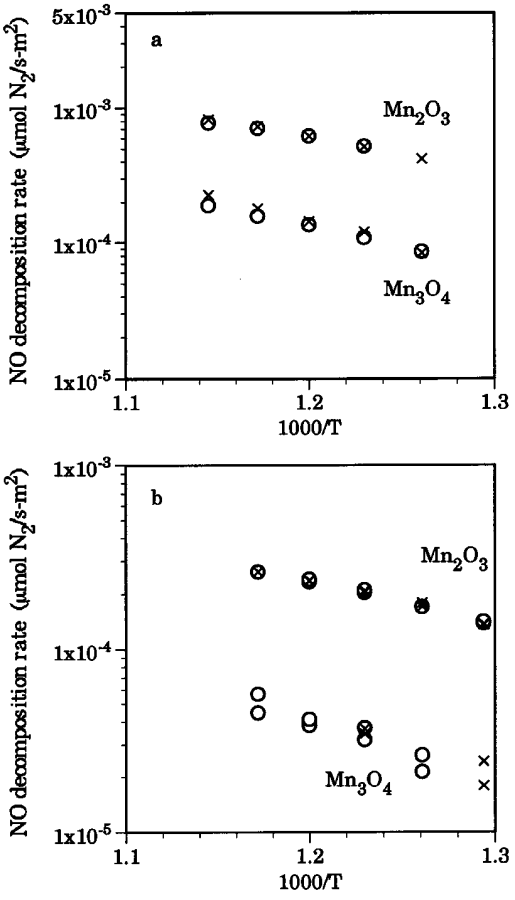

FIG. 4. Arrhenius plots for NO decomposition over Mn_2O_3 and Mn_3O_4: (a) $P_{NO} = 0.04$ atm, (b) $P_{NO} = 0.02$ atm; (○) ascending temperature, (×) descending temperature.

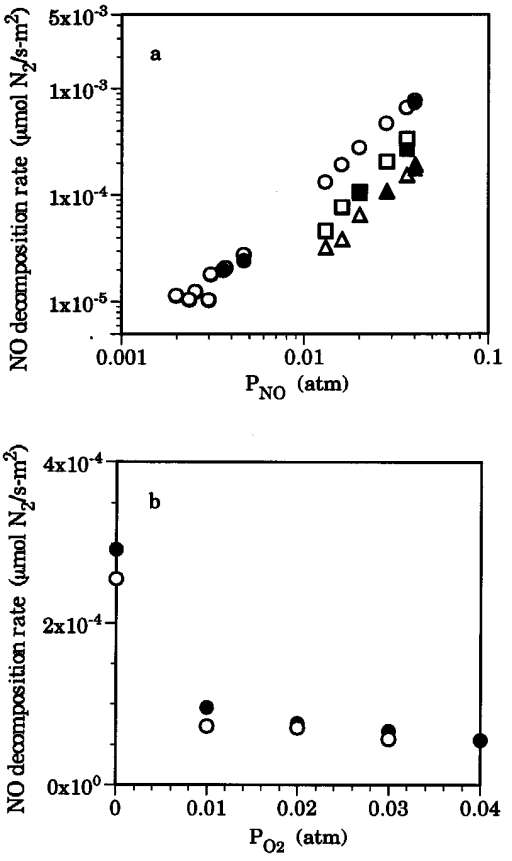

FIG. 5. NO decomposition at 873 K. (a) NO pressure dependencies: Mn_2O_3 (○, ●) No O_2 in feed, (□, ■) $P_{O_2} = 0.01$ atm in feed; NO over Mn_3O_4 (△, ▲) No O_2 in feed; (b) O_2 pressure dependency (○, ●); $P_{NO} = 0.02$ atm. Solid symbols, ascending P_{O_2}; open symbols, descending P_{O_2}.

observed, as indicated by Fig. 5a. Based on a power rate law expression, the reaction order with respect to NO was 1.5 for Mn_2O_3 and 1.6 for Mn_3O_4. Table 2 summarizes the activities and kinetic parameters for Mn_2O_3 and Mn_3O_4. The effect of O_2 partial pressure on the rate of NO decomposition was also examined for Mn_2O_3 at 873 K and 0.02 atm of NO by first increasing O_2 pressure then decreasing it. A greater extent of catalyst deactivation was observed than

TABLE 2

Activities and Kinetic Parameters for NO Decomposition over Mn_2O_3 and Mn_3O_4 ($T = 773$ K)

Catalyst	P_{NO} (atm)	E_a (kcal/mole)	Rate (μmole N_2/s/g)	Specific activity (μmole N_2/s/m^2)
Mn_2O_3	0.04	11[a]	9.5×10^{-3}	3.5×10^{-4}
	0.02	11[b]	3.9×10^{-3}	1.4×10^{-4}
Mn_3O_4	0.04	15[a]	9.5×10^{-4}	6.5×10^{-5}
	0.02	15[b]	2.8×10^{-4}	2.1×10^{-5}

[a] 793–873 K.
[b] 773–853 K.

TABLE 3

Reaction Orders with Respect to NO and O_2 for NO Decomposition

Catalyst	Temperature (K)	NO[a]	NO[b]	O_2[c]
Mn_2O_3	833	1.4	1.6	−0.4
	853	1.5	1.9	−0.3
	873	1.5	1.8	−0.3
Mn_3O_4	873	1.6	—	—

[a] No O_2 in the feed gas.
[b] 0.01 atm of O_2 in the feed gas.
[c] $P_{NO} = 0.02$ atm.

in the experiments without O_2 in the feed. As shown in Fig. 5b, an inhibitory effect of O_2 was observed and the rate with 0.04 atm of O_2 was lower by a factor of four than that with no O_2 in the feed. The reaction order on O_2 was −0.3 above 0.01 atm O_2. The reaction orders on NO in the presence (0.01 atm) and absence of O_2 were also examined at 873 K, and Fig. 5a shows that the reaction order on NO is somewhat greater in the presence of O_2 than in its absence. Similar experiments were used to obtain reaction orders with respect to NO and O_2 at 833 and 853 K (5), and the results are summarized in Table 3.

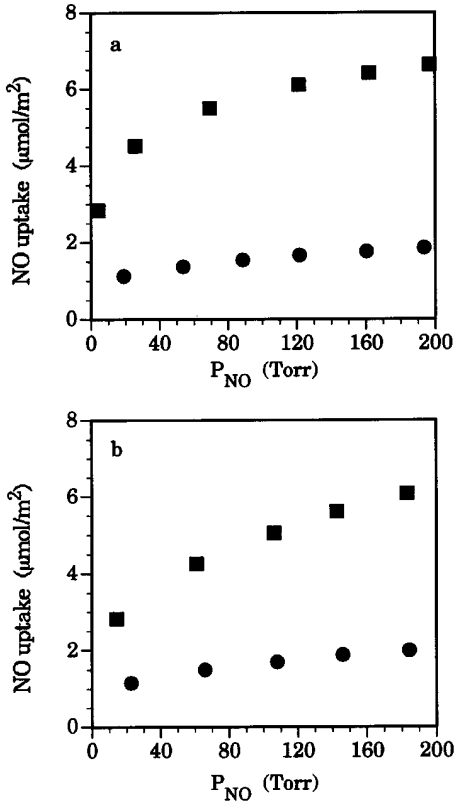

FIG. 6. Chemisorption of NO on (a) Mn_2O_3 (29.2 m^2/g) and (b) Mn_3O_4 (18.3 m^2/g) at 295 K; (■) initial uptake; (●) reversible uptake.

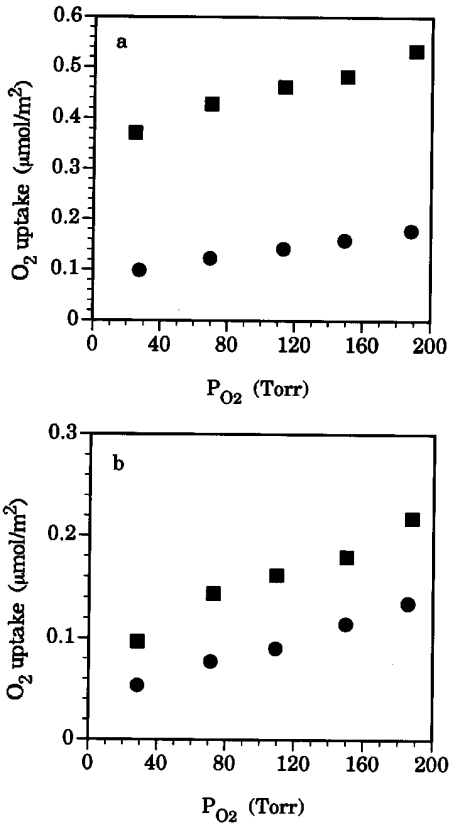

FIG. 7. Chemisorption of O_2 on (a) Mn_2O_3 (31.1 m^2/g) and (b) Mn_3O_4 (18.3 m^2/g) at 295 K; (■) initial uptake; (●) reversible uptake.

Figure 6 shows adsorption isotherms for NO on Mn_2O_3 and Mn_3O_4, and Fig. 7 shows the isotherms for O_2, all measured at 295 K. The NO uptakes by both catalysts were substantial, but the final rate of adsorption was slow, which indicated possible activated chemisorption. Irreversible uptakes of NO were determined by the dual isotherm method, and all values for irreversible NO chemisorption were obtained at 200 Torr. The irreversible uptakes of O_2 on Mn_2O_3 and Mn_3O_4 were 0.19×10^{18} and 0.04×10^{18} molecule O_2/m^2, respectively, and these uptake values, which were independent of pressure, are also listed in Table 1.

DISCUSSION

Early studies of catalytic NO decomposition date back to almost the beginning of the century (8), and numerous reviews are available on this subject (2, 3, 9–14). In the 1960s and early 1970's, NO decomposition was investigated in some detail over metal and simple binary oxides (15–22). Winter examined dozens of metal oxides as catalysts for this reaction, although no data with Mn oxides were obtained, and he proposed a rate expression which incorporated an inhibitory effect of O_2 on the rate of NO decomposition, which had been suggested previously (15). However,

the inhibitory effect of O_2 had never been tested explicitly until Amirnazmi *et al*. investigated the catalytic activity of Pt/Al_2O_3 and several metal oxides for NO decomposition by adding O_2 to the feed gas (16). Their quantitative investigation found strong inhibition of O_2 with all the catalysts tested, and it clearly established the inhibitory effect. Later studies have always observed this effect, regardless of the catalyst used, and it has been unanimously agreed both that O_2 retards NO decomposition and that oxygen lability at the catalyst surface is important. When studies of catalytic NO decomposition were reviewed in 1975 by Hightower and van Leirsburg (10) and Shelef (11), Co_3O_4 was deemed to be the most active material, but its activity was several orders of magnitude lower than the level needed for commercial applications (19).

Subsequent studies branched into the investigation of two major classes of catalysts—mixed oxides and zeolites. Hamada *et al*. found that Ag considerably promoted the activity of Co_3O_4 and at the same time alleviated the inhibitory effect of O_2, and they speculated that the active surface species was some complex of Co and Ag (23). Voorhoeve pointed out that the stability of mixed metallic valence states in the perovskite structure and the mobility of oxygen ions should make perovskite-type compounds promising as catalysts (24). Uchijima examined the activity of various perovskite compounds (25), while Shimada et al. (26) and Tabata *et al*. (27) studied Y–Ba–Cu–O-type oxides. Some K_2NiF_4-type and perovskite-type oxides were examined by Teraoka *et al*. (28) and Yasuda *et al*. (29, 30). Although some of them showed appreciable specific activity and possessed good structural stability at high temperatures, their activity on a weight basis was only moderate due to their low surface area (30). Iwamoto and co-workers first investigated the activity of zeolites for NO decomposition starting with Cu-Y zeolites and found Cu-ZSM-5 is extremely active, i.e., three to four orders of magnitude more active than the most active Co_3O_4 (32). Subsequent studies on Cu-ZSM-5 revealed that an excessively ion exchanged form of Cu-ZSM-5 is most active (33); however, even this level of activity appears to be insufficient for commercial use (34). Later studies found that Cu-ZSM-5 also exhibits high activity for NO reduction using hydrocarbons as reducing agents (35, 36).

Few papers have been published on NO decomposition over Mn oxides. Yur'eva *et al*. found that NO decomposition over MnO_2 at 293, 323, and 573 K apparently produced only NO_2, which was trapped, and no kinetic data were reported (17). Winter remarked that MnO_2 showed some activity, which was not given quantitatively, at temperatures well above 623 K but it decomposed *in vacuo*, and Mn_2O_3 gave no reproducible results; thus no data were again provided (15). Edwards and Harrison examined NO decomposition over Mn_3O_4 at around 500 K and 1 ppm of NO in air using a flow reactor and, from their apparent activation energy and the preexponential factor, they suggested that Mn_3O_4 would be several times more active than other catalysts reported at that time (37)). In fact, extrapolation of their data at 516 K and 1.2 ppm of NO to the reaction conditions of the present study, i.e., 773 K and 0.04 atm NO, gives an activity of 230 μmol $N_2/s \cdot g$, which is orders of magnitude higher than the present results, and the Mn_3O_4 used here failed to show observable activity at 516 K, even with 0.04 atm of NO. No N_2 formation was reported, and it is almost certain that either the rate of oxidation of Mn_3O_4 by NO or the activated adsorption of NO on Mn_3O_4 (or both) was measured rather than a catalytic reaction. Other studies with Mn oxides include NO reduction by CO, H_2, and NH_3 over MnO (38), MnO_2 (39, 40), Mn oxides and supported Mn oxides (41, 42), and a mixture of Pt/SiO_2 and Mn_2O_3 (43). The stoichiometric reaction of NO with reduced MnO_2 to reoxidize it was examined (44), and NO reduction by C_3H_6 over an Mn_2O_3/zeolite mixture has been studied (45). These latter investigations differ from the direct catalytic decomposition of NO.

Since no quantitative work has been reported over Mn oxides, the catalytic activities of Mn_2O_3 and Mn_3O_4 determined in this study shall be compared to those of other relevant oxide catalysts. Before that, however, some discussion is in order to clarify why no O_2 was observed in the product gas when NO decomposition was carried out without O_2 in the feed. This phenomenon has been reported by many researchers during NO decomposition over metal oxides and zeolites and has been attributed to the reaction: $2NO + O_2 \rightarrow 2NO_2$, which occurs in a room-temperature region downstream form the reactor (15). This is reasonable considering that the rate of this homogeneous gas-phase reaction to form NO_2 can be expressed as $r = k[O_2][NO]$ (46), and the equilibrium constant, K_p, equals 2.43×10^{12} at 298 K, which is much in favor of NO_2, whereas $K_p = 0.82$ at 773 K. Li and Hall carried out NO decomposition over Cu-ZSM-5 and found that when conversions of NO were above ~45%, O_2 in the product could be analyzed accurately by GC and the O_2/N_2 ratio in the product increased monotonically with conversion to reach unity at 100% conversion (47). This behavior clearly showed formation of NO_2 by the reaction between unreacted NO and product O_2 in the postreactor line. In the present study the NO_2 concentration in the product gas was monitored by a NO_x analyzer to confirm the stoichiometric decomposition of NO over Mn_2O_3 and Mn_3O_4. From the reaction stoichiometry ($2NO + O_2 = 2NO_2$) and the NO_2 concentration measured in the effluent stream, the O_2 concentration in the product stream could be calculated assuming no reaction to NO_2. Ideally it is the same as the N_2 concentration, and this linear relationship was indeed obtained although the O_2 concentration fell 10–15% below the linear plot above 1000 ppm N_2 (5).

The NO decomposition activities of various oxide catalysts have been extracted from previous work when possible

TABLE 4

Catalytic Behavior for NO Decomposition over Oxide Catalysts ($P_{NO} = 0.04$ atm)

Catalyst	Temp. (K)	E_a (kcal/mol)	Activity[a] (μmol N_2/ s · g × 10^4)	Activity[a] (μmol N_2/ s · m^2 × 10^5)	Reference
Mn_2O_3	773	11	95	36	This study
Mn_3O_4	773	15	10	7	This study
La_2O_3	773	23	8	23	56
Co_3O_4	773	28	260	320	19
Co_3O_4	773	—	420	—	23
Ag/Co_3O_4	773	—	2,000	—	23
$La_{1.5}Sr_{0.5}CuO_4$	773	26	18	200	30
$LaMn_{0.6}Cu_{0.4}O_3$	773	1	90	370	30
Cu-ZSM-5	773	22	120,000	—	48
Mn_2O_3	873	11	220	80	This study
Mn_3O_4	873	15	29	21	This study
CuO	873	8	—	24	16
La_2O_3	873	23	45	130	56
Co_3O_4	873	28	—	1000	16
Fe_2O_3	973	—	—	8	16
NiO	973	—	—	12	16
CuO	973	8	—	390	16

[a] When necessary, rates were extrapolated to 0.04 atm NO assuming a first-order pressure dependence on NO.

and are listed in Table 4. If rate data at 0.04 atm were not available, the rates were extrapolated to this pressure assuming a first-order dependence on NO. Amirnazmi *et al.* studied NO decomposition over Pt/Al_2O_3 and different metal oxides in a fixed-bed reactor. Having observed a strong inhibitory effect of O_2 for all the catalysts they tested, they realized the difficulty of comparing rate data at different conversion levels of NO and decided to use rate data at zero partial pressure of O_2, which were obtained by extrapolation using the observed linear dependence of the inverse rate upon the partial pressure of O_2 (16). However, applying this method to other catalysts is debatable and at low conversions of 10% or less the errors will not be unacceptably large; consequently, no corrections were made to the data in Table 4, and thus they reflect the effect of O_2. As a result, the activities from Amirnazmi *et al.* are somewhat overestimated while the rates from Hamada *et al.* (23) are somewhat underestimated because they represent rate data at high conversions (17–45%). The rate data in Table 4 show that Cu-ZSM-5 (48) is overwhelmingly more active than the others, and its activity is followed by Ag/Co_3O_4 and Co_3O_4 (23). K_2NiF_4-type mixed oxides, $La_{1.5}Sr_{0.5}CuO_4$ and $LaMn_{0.6}Cu_{0.4}O_3$ are more active than Mn_2O_3 on a surface area basis (30), but similar on a weight basis because their surface areas are small. Within the group of simple binary oxides, the specific activity of Mn_2O_3 is less than that of Co_3O_4, similar to that of La_2O_3, and higher than those of CuO, NiO, and Fe_2O_3 (16). As to the apparent activation energies, the respective values of 11 and 15 kcal/mol for Mn_2O_3 and Mn_3O_4 are relatively low compared to those for the other catalysts listed in Table 4. The apparent activation energies for the dozens of oxides catalysts reviewed by Hightower and van Leirsburg range from 10 to 40 kcal/mol (10), which again shows that the E_a values for Mn_2O_3 and Mn_3O_4 are relatively low.

While homogeneous NO decomposition seems to proceed with a second-order dependence on NO (49), reported reaction orders with respect to NO for the catalytic decomposition of NO have varied from zero to two (10). A zero-order dependence on NO pressure has been reported for NO decomposition over metal oxides such as Cr_2O_3 and Fe_2O_3 (50). In contrast, second-order dependences on NO were obtained by Yur'eva *et al.* (17) and Sakaida *et al.* (18) for this reaction over various metal oxides. On the other hand, first-order kinetics were obtained over Co_2O_3 and CuO by Sourirajan and Blumenthal (20), which was later confirmed by Shelef *et al.* (19). Winter proposed first-order kinetics for many metal oxides (15), and Amirnazmi *et al.* determined first-order NO dependencies for NO decomposition over Pt/Al_2O_3 and several metal oxides (16). At the time of their review of catalytic NO decomposition, Hightower and van Leirsburg concluded that there was a general consensus that the reaction was first order in NO (10). After that, however, Iwamoto *et al.* found a reaction order of 1.6 for NO decomposition over a Cu(II)-exchanged Y-type zeolite (51), whereas Li and Hall found a first-order

dependence on NO for NO decomposition over Cu-ZSM-5 (48). In the present case, the reaction orders on NO were found to be clearly and consistently greater than unity for both Mn_2O_3 and Mn_3O_4. With Mn_2O_3 the reaction order was 1.5 at 873 K over a wide range of NO partial pressures from 0.002 to 0.04 atm, and it was always greater with O_2 in the feed gas than in its absence, which seems reasonable for the following reasons. In the absence of O_2 in the feed, the inhibitory effect of O_2 would be imposed only by the O_2 formed during reaction. With other conditions fixed, the amount of O_2 formed would be larger at higher NO partial pressures because of higher rates, hence higher conversions of NO decomposition; thus the inhibitory effect of O_2 can be more pronounced at higher NO partial pressures which can result in lower apparent reaction orders with respect to NO. In the presence of a relatively large amount of O_2 in the feed gas, on the other hand, the O_2 formed by decomposition is small compared to the already existing O_2 partial pressure so that an additional inhibitory effect is not significant. If O_2 competes with NO for adsorption sites, the surface coverage by oxygen has a significant effect.

An inhibitory effect of O_2 upon NO decomposition has been suggested or reported in many papers (10), yet few detailed investigations have quantified it. Amirnazmi *et al.* examined the effect of O_2 partial pressure on the rate of NO decomposition over Pt/Al_2O_3 and Co_3O_4 at 873 K and near atmospheric pressure using an NO concentration of 5% and O_2 concentrations ranging from 1 to 5%, and they calculated reaction orders with respect to O_2 of -0.6 for Pt/Al_2O_3 and -0.8 for Co_3O_4 (16). In their study of NO decomposition over Cu/ZSM-5, Li and Hall determined reaction orders for O_2 of -0.22 to -0.44 which increased as the temperature decreased from 823 to 723 K (48). As given in Table 3, the reaction orders of O_2 observed in the present study were -0.3 to -0.4 under reaction conditions similar to those used by Amirnazmi *et al.*, which indicates a somewhat smaller inhibitory effect of O_2 for Mn_2O_3 compared to their catalysts.

Various rate expressions and pertinent reaction mechanisms have been proposed in the literature. The rate expressions have been either first- or second-order in NO, and all of them contain an O_2-related term to incorporate the inhibitory effect of O_2. Winter thought that oxygen vacancies are important and proposed that a pair of adjacent F-centers, each designated as an electron bound to an oxygen vacancy, was the active site. Based on the observed first-order NO dependence for its decomposition over various metal oxides, he proposed rapid adsorption of the initial NO molecule followed by a rate-determining step associated with the adsorption of a second NO molecule on the adjacent open F-center. His mechanism led to a rate expression of the form, $r = aP_{NO}/(1 + bP_{O_2})$, where a and b are constants (15). Having also observed first-order kinetics for NO decomposition over Pt/Al_2O_3 and several metal oxides, Amirnazmi *et al.* concluded that a rate expression of the same form as Winter's could adequately represent their experimental data (16), and such a rate expression was obtained by assuming that the adsorption of NO on a site, designated as *, was one of three slow steps and the concentration of the most abundant surface species, O^*, was governed by the equilibrium: $O_s + O* \rightleftharpoons O_2 + *$, where O_s is a mobile surface oxygen atom (52), as shown below:

$$\begin{aligned} &NO + * \rightarrow NO* \\ &NO + NO* \rightarrow N_2O + O* \\ &N_2O \rightarrow N_2 + O_s \\ &O_s + O* \rightleftharpoons O_2 + *. \end{aligned}$$

No explanations or suggestions were made on the nature of the surface site and the distinction between O^* and O_s. Hall and co-workers obtained a somewhat different rate expression, i.e., $r = aP_{NO}/(1 + bP_{O_2}^{1/2})$, based on their study with Cu-ZSM-56 (48, 53). The model assumed that extra lattice oxygen atoms represented reaction centers, designated as O^*, and postulated a dinitrosyl-type intermediate, $[^*NO_2NO]$, which decomposes into N_2 and O_2 and regenerates the O^* site. Sakaida *et al.* found that a rate expression of the form $r = P_{NO}^2/(1+bP_{O_2}^{1/2})^2$ fit their experimental data over $Pt–Ni/Al_2O_3$ well, and they suggested a three-step sequence which included a reaction between two adsorbed NO molecules (18). Although numerous rate expressions have been proposed, including some not mentioned above (10), constants in these expressions have seldom been determined and only Boudart and co-workers have assessed their reasonableness (16, 52). The maximum first-order dependence of the first two rate expressions clearly eliminates them as candidates to describe the near second-order kinetics observed in our study.

Examination of the detailed kinetic data with Mn_2O_3 suggests that NO decomposition over Mn_2O_3 proceeds via a second-order, rate-determining surface reaction between NO molecules or NO-related intermediates, with retardation effects by O_2 or oxygen-related intermediates. With this perspective the following Langmuir–Hinshelwood (L-H) model can be proposed, where * denotes an active site:

$$\begin{aligned} &2[NO + * \overset{K_{NO}}{\rightleftharpoons} NO*] \\ &2NO* \overset{k}{\rightarrow} N_2 + 2O* \quad \text{(rds)} \quad \text{or} \quad \left\{ \begin{array}{l} 2NO* \rightarrow N_2O* + O* \\ N_2O* \rightarrow N_2 + O* \end{array} \right\} \\ &2O* \overset{1/K_{O_2}}{\rightleftharpoons} O_2 + 2* \\ &\hline \\ &2NO \rightarrow N_2 + O_2. \end{aligned}$$

The first step represents quasi-equilibrated NO adsorption followed by a rate-determining bimolecular surface reaction between adsorbed NO molecules to produce N_2 and

oxygen. The third step is the regeneration of active sites by O_2 desorption. It is possible that the second step involves the formation of N_2O and its rapid decomposition, as shown in brackets, because N_2O was observed by mass spectroscopy when NO was contacted with freshly pretreated Mn_2O_3 at 300 K (54). The same experiment conducted at 573 K produced much less gas-phase N_2O, which implies rapid decomposition of N_2O at the higher temperatures. A rate of 0.60 μmole N_2/s/m^2 for N_2O decomposition at 873 K and 0.04 atm N_2O can be estimated using the rate expression developed in a previous study (4); this rate is 700 times greater than the rate of NO decomposition at 873 K and 0.04 atm of NO, i.e., 8.1×10^{-4} μmol N_2/s/m^2. If the concentration of N_2O^* is very low compared to other surface species, which is reasonable because the adsorption of N_2O on Mn_2O_3 is weak even at 300 K (4), and if the total concentration of active sites, L, is constant, the following L-H rate expression can be easily derived from a site balance assuming only adsorbed NO molecules and O atoms need to be considered. If θ_{NO} is the coverage of NO and $k' = Lk$, then

$$r = Lk\theta_{NO}^2 = \frac{k' K_{NO}^2 P_{NO}^2}{\left(1 + K_{NO} P_{NO} + K_{O_2}^{1/2} P_{O_2}^{1/2}\right)^2}. \qquad [1]$$

The L-H expression embodies a reaction order up to two for NO and the inhibitory effect of O_2. The rate-determining step could be the formation of N_2O, followed by its rapid decomposition into N_2, but this sequence gives the same rate expression as above. Other models were examined, such as the three previously mentioned plus those invoking a unimolecular decomposition of the surface NO species as a rate determining step, but were discarded because they were inconsistent with the experimental results (5). The model involving the quasi-equilibrated formation of a surface $(NO)_2^*$ species via gas-phase and adsorbed NO molecules is a possibility and is discussed elsewhere (54), but the model proposed here is the simplest that gives a meaningful fit of the data.

The derived, three-parameter rate expression was fitted to the experimental data using a nonlinear regression scheme, i.e., the Gauss–Newton iterative technique, under the conditions that the three parameters be positive and the convergence criterion be 10^{-8} (5). Figure 8 shows that an excellent fit between the model and the experimental data for NO is obtained, while Fig. 9 shows a less accurate, but still satisfactory fit for the O_2 dependence with a maximum deviation of 30% at the lowest rate where the most significant analytical errors are expected. The kinetic and thermodynamic parameters obtained from the fitting procedure are listed in Table 5 and have reasonable dependencies; i.e., the rate constant increases and the equilibrium adsorption constants decrease as temperature increases. From these parameters at different temperatures, the activation energy for the rate determining step, E_a, and

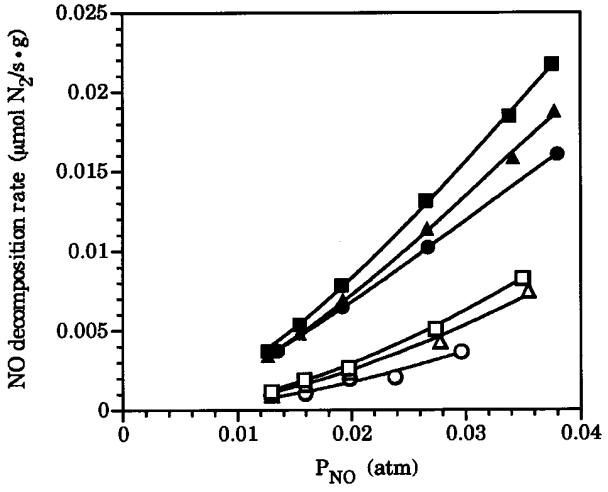

FIG. 8. Fit between model and experimental data for NO decomposition over Mn_2O_3. No O_2 in the feed: (●) 833 K, (△) 853 K, (■) 873 K; 0.01 atm O_2 in the feed: (○) 833 K, (△) 853 K, (□) 873 K.

the enthalpy and entropy of adsorption for NO and O_2, ΔH_{ad}^o and ΔS_{ad}^o, were determined as shown in Fig. 10. The activation energy obtained is 46 kcal/mol, which is higher than that of 31 kcal/mol for N_2O decomposition on Mn_2O_3, thus perhaps reflecting the higher bond strength in the NO molecule. For NO adsorption, ΔH_{ad}^o was -25 kcal/mol and ΔS_{ad}^o was -25 cal/mol/K, and for O_2 adsorption, ΔH_{ad}^o was -35 kcal/mol, and ΔS_{ad}^o was -31 cal/mol/K. Both ΔS_{ad}^o values satisfy the criteria for ΔS_{ad}^o proposed by Boudart *et al.* (55) and Vannice *et al.* (56). Higher ΔH_{ad}^o values for NO adsorption than for N_2O adsorption are consistent with the respective chemisorption behavior, and the *apparent* activation energy for NO decomposition is lower than for N_2O

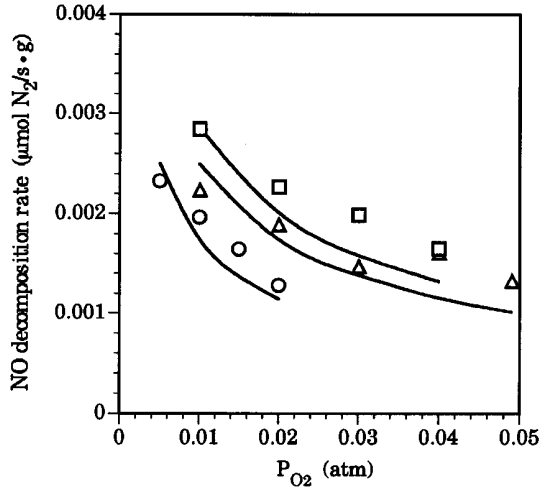

FIG. 9. Fit between model and experimental data for NO decomposition over Mn_2O_3. $P_{NO} = 0.02$ atm in the feed: (○) 833 K, (△) 853 K, (□) 873 K.

TABLE 5

Parameters from Kinetic Rate Expression (Eq. [1])

		Temperature		
		833 K	853 K	873 K
K_{NO}	(atm^{-1})	12.2	7.86	6.18
k'	($\mu mol/s/m^2 \times 10^3$)	9.37	19.0	33.4
K_{O_2}	(atm^{-1})	279	113	107

partly because this higher ΔH^o_{ad} value appears in the numerator of the rate expression. The ΔH^o_{ad} and ΔS^o_{ad} values for O_2 adsorption on Mn_2O_3 are also higher for NO decomposition than for N_2O decomposition, which seems reasonable because at the higher temperatures needed for NO decomposition, a stronger interaction is required between oxygen and the catalyst surface for adsorption. It is also possible that different active sites are involved, however.

Although no one has yet unambiguously identified the active sites for NO decomposition on metal oxides, there seems to be a consensus that they are related to oxygen vacancies (10). Such vacancies can create co-ordinatively unsaturated cations, as well as F-centers, and the former may well be the active sites, as discussed elsewhere (54). Oxygen vacancies must have been produced on Mn_2O_3 and Mn_3O_4 by the pretreatment at 873 K because as many as 6.1×10^{18} and 2.2×10^{18} molecules O_2/m^2 were released from Mn_2O_3 and Mn_3O_4, respectively, during the pretreatment, as shown in Table 1. However, a much smaller amount of O_2 chemisorbed at 300 K, i.e., 0.19×10^{18} molecules O_2/m^2 on Mn_2O_3 and 0.04×10^{18} molecules O_2/m^2 on Mn_3O_4, presumably because 300 K is not high enough to allow dissociative adsorption and only molecular O_2 chemisorption was measured. Regardless, the higher O_2 uptake on Mn_2O_3 might be related to a higher oxygen vacancy concentration, which results in a higher NO decomposition activity for Mn_2O_3 compared to Mn_3O_4. Chemisorption of NO on the Mn_2O_3 and Mn_3O_4 surfaces at 300 K may be complicated first by the fact that NO can produce N_2O upon contact with freshly pretreated Mn_2O_3 or Mn_3O_4 (54) and second by the observation that a portion of the NO chemisorption was kinetically controlled and thus adsorption equilibrium may not have been achieved. Nevertheless, it is clear that much greater amounts of NO than O_2 are adsorbed on these Mn oxides, and the two sets of NO isotherms for Mn_2O_3 and Mn_3O_4 in Fig. 6 can be viewed as approximately the same; i.e., NO coverages for Mn_2O_3 and Mn_3O_4 gave respective values of 4.7 and 4.1 $\mu mol/m^2$ or 2.8×10^{18} and 2.5×10^{18} molecule/m^2. Consequently, the NO chemisorption results may not tell much about either the difference in specific activity between Mn_2O_3 and Mn_3O_4 or the active sites. Regardless, turnover frequencies (TOFs) can also be calculated based on the NO coverages, and the results are listed in Table 6 together with other relevant values for comparison (48, 57). The TOF values for the two Mn oxides are smaller than those for any of the rare-earth oxides and are much smaller than that for Cu-ZSM-5, although the latter value uses a different basis of Cu loading.

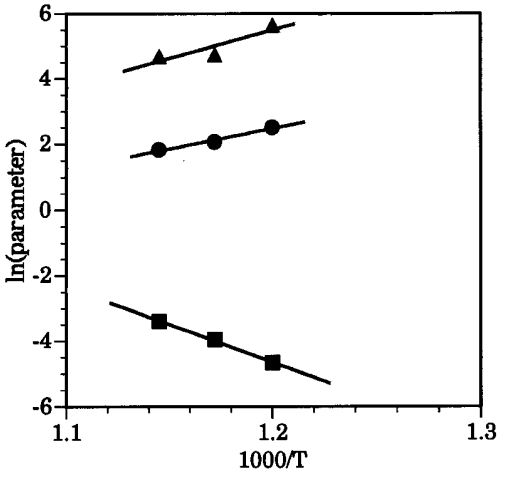

FIG. 10. Dependence of rate parameters on temperature: (●) K_{NO} (atm^{-1}); (■) k' ($\mu mol/s \cdot g$); (△) K_{O_2} (atm^{-1}).

TABLE 6

Specific Activities for NO Decomposition over Oxide Catalysts ($P_{NO} = 0.02$ atm, $T = 773$ K)

Catalyst	Specific activity ($\mu mol\ N_2/s \cdot m^2 \times 10^3$)	TOF[a] ($s^{-1} \times 10^4$)	Reference
Mn_2O_3	0.14	0.3	This study
Mn_3O_4	0.02	0.05	This study
La_2O_3	0.23[b]	0.6	57
Sr/La_2O_3	0.83	1.4	57
CeO_2	0.22[b]	0.7	57
Nd_2O_3	1.1	4.3	57
Sm_2O_3	1.6	3.6	57
Cu-ZSM-5	—	70[b,c]	48

[a] Based on the irreversible uptake of NO at 300 K.
[b] Extrapolated values.
[c] Based on Cu loading (μmole Cu/g).

SUMMARY

Catalytic decomposition of NO over unsupported Mn_2O_3 and Mn_3O_4 requires temperatures above 773 K for significant rates to occur. During pretreatment in He at 873 K, Mn_2O_3 released more oxygen than Mn_3O_4 and, as with N_2O decomposition, Mn_2O_3 is more active than Mn_3O_4, with the activity difference more pronounced for NO decomposition. Much higher reaction temperatures are required for NO decomposition to achieve a level of activity similar to that for N_2O decomposition, and this may reflect

the much higher N–O bond energy in NO. Comparison of activities with other catalysts showed that Mn_2O_3 is far less active than Cu-ZSM-5, substantially less active than Co_3O_4, nearly as active as La_2O_3, and more active than other simple binary oxides including Mn_3O_4, CuO, Fe_2O_3, and NiO. Detailed kinetic studies demonstrated that the reaction order with respect to NO is near 1.5 with no O_2 in the feed, but increases to around 1.8 with O_2 present. O_2 inhibits the decomposition of NO more strongly than N_2O decomposition and, unlike N_2O, substantial NO chemisorption occurs on Mn_2O_3 at 300 K. A Langmuir–Hinshelwood model involving a surface reaction between two NO molecules fits the kinetic data well and gives reasonable model parameters which provide adsorption enthalpy and entropy values consistent with thermodynamic criteria.

ACKNOWLEDGMENTS

We thank Chemetals and Mobil Corporation for partial support of this study. T.Y. thanks Lion Akzo Co., Ltd., for a grant to study at Penn State.

REFERENCES

1. Argento, V. K., *Chem. Eng. Prog.* **84**, 50 (1988).
2. Armor, J. N., *Appl. Catal. B* **1**, 221 (1992).
3. Iwamoto, M., and Mizuno, N., *Shokubai* **32**, 462 (1990).
4. Yamashita, T., and Vannice, M. A., *J. Catal.* **161**, 254 (1996).
5. Yamashita, T., Ph.D. Thesis, The Pennsylvania State University, 1996.
6. Weisz, P., *Z. Phys. Chem.* **11**, 1 (1957).
7. Yao, H. C., and Shelef, M., *J. Catal.* **31**, 377 (1973).
8. Jellinek, K., *Z. Anorg. Allgem. Chem.* **49**, 229 (1906).
9. Shelef, M., and Kummer, J. T., *Chem. Eng. Prog. Symp. Ser.* **67**, 74 (1971).
10. Hightower, J. W., and van Leirsburg, D. A., *in* "The Catalytic Chemistry of Nitrogen Oxides" (R. L. Klimisch, and J. G. Larson, Eds.), p. 63. Plenum, New York, 1975.
11. Shelef, M., *Catal. Rev.–Sci. Eng.* **11**, 1 (1975).
12. Harrison, B., Wyatt, M., and Gough, K. G., "Catalysis," Vol. 5, p. 127. Royal Soc. Chem., Burlington House, London, 1982.
13. Bousch, H., and Jansen, F., *Catal. Today* **2**, 369 (1988).
14. Iwamoto, M., and Yahiro, H., *Catal. Today* **22**, 5 (1994).
15. Winter, E. R. S., *J. Catal.* **22**, 158 (1971).
16. Amirnazmi, A., Benson, J. E., and Boudart, M., *J. Catal.* **30**, 55 (1973).
17. Yur'eva, T. M., Popovski, V. V., and Boreskov, G. K., *Kinet. Catal.* **6**, 941 (1965).
18. Sakaida, R. R., Rinker, R. G., Wang, Y. L., and Corcoran, W. H., *Am. Inst. Chem. Eng. J.* **7**, 658 (1961).
19. Shelef, M., Otto, K., and Gandhi, H., *Atmos. Environ.* **3**, 107 (1969).
20. Sourirajan, S., and Blumenthal, J. L., "Proceedings, 2nd International Congress on Catalysis, Paris 1960." Technip, Paris, 1960.
21. Winter, E. R. S., *J. Catal.* **34**, 440 (1974).
22. Amirnazmi, A., and Boudart, M., *J. Catal.* **39**, 383 (1975).
23. Hamada, H., Kintaichi, Y., Sasaki, M., and Ito, T., *Chem. Lett.* 1069 (1990).
24. Voorhoeve, R. J. H., *in* "Advanced Materials in Catalysis" (J. J. Burton and R. L. Garten, Eds.), p. 129. Academic Press, New York, 1977.
25. Uchijima, T., *Hyomen* **18**, 132 (1980).
26. Shimada, H., Miyama, S., and Kuroda, H., *Chem. Lett.* 1797 (1988).
27. Tabata, K., Kukuda, H., Kohiki, S., Mizuno, N., and Misono, M., *Chem. Lett.* 799 (1988).
28. Teraoka, Y., Fukuda, H., and Kagawa, S., *Chem. Lett.* 1 (1990).
29. Yasuda, H., Mizuno, N., and Misono, M., *JCS Chem. Commun.* 1094 (1990).
30. Yasuda, H., Nitadori, T., Mizuno, N., and Misono, M., *Nippon Kagaku Kaishi* 604 (1991).
31. Teraoka, Y., Nakano, K., Kagawa, S., and Shangguan, W. F., *Appl. Catal. B* **5**, L181 (1995).
32. Iwamoto, M., Furukawa, H., Mine, Y., Uemura, F., Mikuriya, S., and Kagawa, S., *JCS Chem. Commun.* 1272 (1986).
33. Iwamoto, M., Yahiro, H., Tanda, K., Mizuno, N., Mine, Y., and Kagawa, S., *J. Phys. Chem.* **95**, 3727 (1991).
34. Iwamoto, M., and Hamada, H., *Catal. Today* **10**, 57 (1991).
35. Iwamoto, M., *Shokubai* **32**, 430 (1990).
36. Held, W., Kornig, A., Richter, T., and Puppe, L., SAE paper 900496 (1990).
37. Edwards, H. E., and Harrison, R. M., *Environ. Sci. Technol.* **13**, 673 (1979).
38. Shelef, M., and Otto, K., *J. Catal.* **10**, 408 (1968).
39. Echigoya, E., Niiyama, H., and Ebitani, A., *Nippon Kagaku Kaishi* 222 (1974).
40. Murakami, Y., Hayashi, K., Yasuda, K., and Ito, T., *Nippon Kagaku Kaishi*, 173 (1977).
41. Kapteijn, F., Singoredjo, L., and Andreini, A., *Appl. Catal. B* **3**, 173 (1994).
42. Kapteijn, F., Singoredjo, L., van Driel, M., Andreini, A., Moulijn, J. A., Ramis, G., and Guido, B., *J. Catal.* **150**, 105 (1994).
43. Sakata, K., Uchijima, T., and Yoneda, Y., *Nippon Kagaku Kaishi* 791 (1978).
44. Otsuka, K., *Hyomen* **23**, 206 (1985).
45. Yokoyama, F., and Misono, M., *Shokubai* **36**, 163 (1994).
46. Beattie, I. R., *in* "Comprehensive Treatise on Inorganic and Theoretical Chemistry," Vol. 8, Suppl. II, p. 158. Nitrogen, Longmans, London, 1967.
47. Li, Y., and Hall, W. K., *J. Phys. Chem.* **94**, 6145 (1990).
48. Li, Y., and Hall, W. K., *J. Catal.* **129**, 202 (1991).
49. Wise, H., and Frech, M. F., *J. Chem. Phys.* **20**, 22 (1952).
50. Fraser, J. M., and Daniels, F., *J. Phys. Chem.* **62**, 215 (1958).
51. Iwamoto, M., Yokoo, S., Sakai, K., and Kagawa, S., *J. Chem. Soc. Faraday Trans. I* **77**, 1629 (1981).
52. Lim, K. J., Loffler, D. G., and Boudart, M., *J. Catal.* **100**, 158 (1986).
53. Valyon, J., and Hall, W. K., *J. Phys. Chem.* **97**, 1204 (1993).
54. Yamashita, T., and Vannice, M. A., submitted for publication.
55. Boudart, M., Mears, D. W., and Vannice, M. A., *Ind. Chim. Belge.* **32**, 281 (1967).
56. Vannice, M. A., Hyun, S. H., Kalpacki, B., and Liauh, W. C., *J. Catal.* **56**, 358 (1979).
57. Zhang, X., Walters, B., and Vannice, M. A., *J. Catal.* **155**, 290 (1995).